Concomitant Determination of Absolute Values of Cellular Protein Amounts, Synthesis Rates, and Turnover Rates by Quantitative Proteome Profiling*

Christopher Gerner‡, Susanne Vejda, Dieter Gelbmann, Editha Bayer, Josef Gotzmann, Rolf Schulte-Hermann, and Wolfgang Mikulits

Two-dimensional gel electrophoresis of protein fractions isolated from ^{35}S-radiolabeled cells provides qualitative information on intracellular amounts, ^{35}S incorporation rates, protein modifications, and subcellular localizations of up to thousands of individual proteins. In this study we extended proteome profiling to provide quantitative data on synthesis rates of individual proteins. We combined fluorescence detection of radiolabeled proteins with SYPRO ruby™ staining and subsequent autoradiography of the same gels, thereby quantifying protein amounts and ^{35}S incorporation. To calibrate calculation of absolute synthesis rates, we determined the amount and autoradiograph intensity of radiolabeled haptoglobin secreted by interleukin-6 pretreated HepG2 cells. This allowed us to obtain a standard calibration value for ^{35}S incorporation per autoradiograph intensity unit. This value was used to measure protein synthesis rates during time course experiments of heat-shocked U937 cells. We measured the increasing amounts of hsp70 and calculated it by integration of the determined hsp70 synthesis rates over time. Similar results were obtained by both methods, validating our standardization procedure. Based on the assumption that the synthesis rate of proteins in a steady state of cell metabolism would essentially compensate protein degradation, we calculated biological half-lives of proteins from protein amounts and synthesis rates determined from two-dimensional gels. Calculated protein half-lives were found close to those determined by pulse-chase experiments, thus validating this new method. In conclusion, we devised a method to assess quantitative proteome profiles covering determination of individual amounts, synthesis, and turnover rates of proteins. ***Molecular & Cellular Proteomics 1: 528–537, 2002.***

The ability to monitor variations at the transcriptional and translational levels using DNA microarrays and proteomics is essential to improve our understanding of physiologically relevant processes at a molecular level (1). Current DNA array technologies allow quantitative high throughput analysis of many thousands genes simultaneously. Yet, this analysis is rather confined to steady state mRNA levels, and mRNA abundance does not necessarily reflect the levels of corresponding proteins (2, 3). Protein levels are regulated by post-transcriptional mechanisms including transcript localization (4) and stability (5), translational regulation (6, 7), and protein degradation (8). Therefore, methods to simultaneously determine levels and turnover of the cellular proteins remain an urgent necessity. However, current proteome techniques still lag behind in quantitative high throughput analysis as compared with DNA arrays.

A variety of methods have been developed to quantitatively monitor the protein expression profile of cells. Although protein chips and encoded particle-based solution arrays are particularly encouraging as the next generation proteomics platforms (9, 10), current techniques still largely rely on separation of proteins by high resolution two-dimensional gel electrophoresis (2-DE).[1] Spot quantification may be based on a two-color fluorescent labeling system (11, 12), on dual metabolic labeling with stable isotopes (13, 14), or on post-isolation isotopic protein labeling with isotope-coded affinity tag (15–17). We have demonstrated that combination of metabolic labeling of cells, subcellular fractionation, and subsequent 2D analysis allows us to comprehensively survey alterations in synthesis rates, modifications, and subcellular localization (18). However, all these techniques monitor only relative differences in proteins levels but provide no absolute amounts of the proteins investigated. The development of sensitive fluorescence staining methods provided a new tool to determine absolute protein amounts (19), relying on a linear signal response over a wide dynamic range (20–22).

In this paper we show that combination of metabolic label-

From the Institute of Cancer Research, University of Vienna, 1090 Vienna, Austria

Received, April 23, 2002, and in revised form, June 29, 2002
Published, MCP Papers in Press, July 22, 2002, DOI 10.1074/mcp.M200026-MCP200

[1] The abbreviations used are: 2-DE, two-dimensional gel electrophoresis; CBB, Coomassie Brilliant Blue; CF, calibration factor; CHAPS, 3-[3-cholamidopropyl)dimethylammonio]-1-propanesulfonate; 2D, two-dimensional; FCS, fetal calf serum; hsp, heat shock protein; IL-6, interleukin 6.

ing of cells, 2D electrophoresis, fluorescence staining, and autoradiography allowed us to determine absolute values not only for protein amounts but also for protein synthesis rates and turnover rates. Introducing a standard curve for intracellular, as well as extracellular, proteins we determined absolute protein amounts from SYPRO ruby™-stained gels. To calculate synthesis rates of proteins from autoradiograph intensities of 2D gel spots, we introduced a calibration factor relating the incorporation of 1 pmol of ^{35}S into a protein to a constant value of autoradiograph intensity. We calibrated this measurement by determination of the amount and autoradiograph intensity of radiolabeled secreted haptoglobin. Synthesis rates of proteins expressed in mol per h per cell were hence calculated from the autoradiograph intensity of identified spots. To our knowledge, this is the first time that a method was devised to determine absolute synthesis rates of a large number of proteins within one experiment. Monitoring synthesis and accumulation of hsp70 following heat shock of U937 cells validated absolute protein synthesis profiling. Assuming that the synthesis rate of proteins in a steady state of cell metabolism would essentially compensate protein degradation, we calculated protein turnover rates from absolute protein amounts and synthesis rates. Protein half-lives were determined by measurement of the recovery of spot autoradiograph intensities of pulse-chased cells in comparison to pulsed cells (23). Calculated protein half-lives were found close to those obtained by pulse-chase experiments, thus validating this new method.

EXPERIMENTAL PROCEDURES

Cell Culture—HepG2 (human hepatoblastoma cells) were maintained in minimal essential medium (MEM; Invitrogen) supplemented with 1 mM sodium pyruvate, 1% non essential amino acids (Biochrom AG, Berlin, Germany), and 10% FCS. U937 (human monocyte-like histiocytic lymphoma cells) were routinely cultivated in RPMI 1640, supplemented with 10% FCS at 37 °C in a humidified atmosphere containing 5% CO_2.

IL-6 Treatment of HepG2 Cells and Metabolic Labeling—Confluent HepG2 cells were treated with or without IL-6 at 50 ng/ml (Strathmann Biotec AG, Dengelberg, Germany) for 24 h. Subsequently, cells were washed and reseeded in methionine-free medium (ICN) supplemented with 0.2 mCi/ml ^{35}S protein labeling mix. After 1 h, cells were washed and incubated again with methionine-free medium supplemented with 0.2 mCi/ml ^{35}S protein labeling mix for 1 h. Then, the supernatant was collected and sterile-filtrated to remove cellular debris, and the protein was precipitated by the addition of ethanol. After 24 h at −20 °C, precipitated proteins were pelleted, dried, and solubilized in 2D sample buffer (10 M urea, 4% CHAPS, 0.5% SDS, 100 mM dithiothreitol). The labeling mix contained labeled methionine and cysteine; however, labeling occurred in the presence of an excess of unlabeled cysteine. Therefore, only the contribution of methionine to radiolabeling of proteins was considered, whereas that of cysteine was disregarded.

Heat Shock and Metabolic Labeling—For heat shock, U937 cells were incubated for the times indicated in a water bath preset to the respective temperature. After 2, 6, or 10 h, cells were washed and re-seeded at a density of 10^6 cells/ml in methionine-free medium (ICN) supplemented with 10% FCS and ^{35}S protein labeling mix (ICN) at 0.8 mCi/10^7 cells and labeled for 2 h. Afterward, cells were washed twice with phosphate-buffered saline and fractionated. Aliquots of labeled cells, which were regarded as controls, were not heat-shocked. One cell aliquot was first labeled, then heat-shocked, and processed further immediately afterward. For the pulse-chase experiment, one aliquot of labeled control cells was washed, counted, cultivated under standard conditions for another 24 h, counted again, and then harvested. All data were reproduced.

Subcellular Fractionation—All buffers were supplemented with protease inhibitors phenylmethylsulfonyl fluoride (1 mM), aprotinin, leupeptin, and pepstatin A (each at 1 μg/ml). Cells were lysed in 0.05% Nonidet P-40 in hypotonic buffer (10 mM Hepes/NaOH, pH 7.4, 10 mM NaCl, 3 mM $MgCl_2$). Nuclei were pelleted at 400 g for 10 min, and the resulting supernatant was centrifuged at 100,000 × *g* for 60 min to get the supernatant S-100 fraction. After ethanol precipitation, the pelleted cytoplasmic protein fraction enriched in organelles except nuclei and membranes was directly solubilized in sample buffer.

Two-dimensional Electrophoresis, SDS-PAGE, Fluorography, and Autoradiography—High resolution two-dimensional gel electrophoresis was carried out as described previously (18), using the Protean II xi electrophoresis system (Bio-Rad). The protein samples were dissolved in sample buffer supplemented with 2% (w/v) ampholyte, pH 7–9 (BDH). To optimize solubilization of proteins, we saturated the protein solution with urea by addition of solid urea. Isoelectric focusing of protein samples was performed at 15,500 V-h in a stepwise fashion (2 h at 200 V, 3 h at 500 V, 17 h at 800 V) at an acrylamide concentration of 4% T (Gerbu, Gaiberg, Germany)/0.1% C (piperazine diacrylamide; Bio-Rad) in 1.5-mm × 16-cm tube gels. The gel buffer contained 0.035% Nonidet P-40, 0.1% CHAPS, and 2% ampholytes (Merck) (1 vol. pH 3.5–10/1 vol. pH 4–8/2 vol. pH 5–7). Degassed 20 mM NaOH served as catholyte, and 6 mM H_3PO_4 served as an anolyte. For SDS-PAGE, the extruded tube gels were placed on top of 1.5-mm 12% T polyacrylamide slab gels. Tube gels were overlaid with equilibration buffer (2.9% SDS, 70 mM Tris-HCl, pH 6.8, 0.001% bromphenol blue), and after 3 min the gels were run at 15 °C in electrode buffer (0.1% SDS, 25 mM Tris base, 192 mM glycine). Gels were stained with 0.25% Coomassie Brilliant Blue R 250 (Sigma), silver-stained by the method of Wray *et al.* (24), or stained with SYPRO ruby™ (Molecular Probes). To enhance the SYPRO ruby™ staining, proteins were cross-linked using 5% glutaraldehyde/1 mM dithiothreitol. After washing the gels four times with water, SYPRO ruby™ staining was performed essentially according to the manufacturers' instructions. Fluorography scanning was performed with the FluorImager 595 (Molecular Dynamics) at a resolution of 200 μm. After scanning, gels were equilibrated for 20 min with Enlightening NEF974G (PerkinElmer Life Sciences) in the case of ^{35}S autoradiography. Then gels were laid on Whatman 3MM chromatography paper, covered with Saran wrap, and dried at 60 °C using the Slab Gel Dryer SE1160 from Hoefer (San Francisco, CA). Exposition of BIOMAX™MR x-ray films (Kodak) in autoradiography cassettes with amplifying screens and of Storage Phosphor Screens (Molecular Dynamics) occurred at room temperature for 48 h. Screens were subsequently scanned with the PhosphorImager SI (Molecular Dynamics) at a resolution of 200 μm.

To assess unspecific protein precipitation, we isolated protein precipitates formed on the top of a tube gel (derived from basic proteins not entering the isoelectric focusing gel) after isoelectric focusing, solubilized them again, and analyzed it by 2-DE. By this means we found that loading up to 200 μg of protein on a 1.5-mm tube gel did not result in unspecific precipitation, as no protein was detectable in the isoelectric focusing 2D gel of the precipitate. However, loading more than 250 μg of protein or loading protein at concentrations higher than 5 μg/μl resulted in protein loss by unspecific precipitation, as many proteins were then detectable in the isoelectric focusing 2D gel of the precipitate. Therefore, at the conditions employed for this

study, we confirmed that no unspecific protein precipitation occurred.

Evaluation of 2D Data—Scanning of gels, background correction, spot editing, quantification, and comparative evaluation of 2D data was accomplished with the ImageMaster 2D Elite v3.1 software (Amersham Biosciences). S.E. values were determined with GraphPad Prism software (GraphPad Software, San Diego). A calibration curve for fluorography using nonlinear regression (curve fit, B_{max} = 21.000.000, K_D = 1.100.000 applying for a spot of 200 pixels) was generated from the calibration experiment (see Fig. 2) using the GraphPad Prism software. Data files with all essential spot information such as identity, integrated intensity, spot size, and background correction were exported from the ImageMaster software to Microsoft® Excel 2000 to calculate absolute protein amounts and synthesis rates. Thus, the protein amounts were calculated as follows: A [ng] = (PS/200) × (K_D × V_{FL}/(PS/200))/((B_{max} − (V_{FL}/(PS/200))), where A is protein amounts, V_{FL} is fluorographic spot intensities of a spot, and PS is pixel size of a spot. Normalization of quantitative data of the heat shock experiment was performed with respect to the sum of protein amounts detected in a gel, taking the control as reference.

Northern Blot Analysis—30 μg of cytoplasmic RNA from each sample of the U937 time course experiment was analyzed by electrophoresis on denaturing 1% formaldehyde-agarose gels, and subsequent Northern blotting was as described previously (25). After UV cross-linking, transfer of 18 and 28 S rRNAs was visualized by methylene blue staining of filters. The membranes were hybridized with ^{32}P-labeled probes specific for human hsp70 (26). For normalization, filters were rehybridized with an [γ-^{32}P]-end-labeled oligodeoxynucleotide specific for human 28 S rRNA (5′-ACG GGA GGT TTC TGT CCT CCC-3′) as described (27). After washing, hybridized filters were subjected to autoradiography.

RESULTS

Using SYPRO ruby™ Dye for Quantification of Proteins in 2D Gels—Detection of proteins in 2D gels by silver staining is a widely used standard technique because of its high reliability, reproducibility, and sensitivity. However, the staining intensity of a given protein spot does not correlate directly with its protein amount. This can be demonstrated by a comparison of Coomassie Brilliant Blue (CBB), silver staining, and SYPRO ruby™ staining with the corresponding autoradiograph obtained from the same source of radiolabeled proteins (Fig. 1). Note that different amounts of protein, compensating for the different staining sensitivities, were loaded onto the 2D gels shown in Fig. 1 for easier comparison of the resulting protein patterns. Although the amount of stathmin detected was found consistently to exceed that of superoxide dismutase by CBB and SYPRO ruby™ staining, silver staining would erroneously suggest the opposite (Fig. 1). In addition, few proteins, like hnRNP E, were found to be hardly stained at all by silver staining even when present in high amounts (not shown). Although silver staining allows relative quantification of protein spots, determination of absolute protein amounts would require an independent calibration of each single spot. CBB staining does not show such protein-specific alterations in sensitivity, but is generally of low sensitivity, leaving a considerable number of proteins undetectable. To enhance the protein staining sensitivity and linearity of SYPRO ruby™ protein staining, we introduced a protein cross-linking step prior to staining (see "Experimental Procedures"). Fluorographic protein detection using SYPRO ruby™ protein stain was still found not as sensitive as silver staining but much more reliable with respect to protein quantification and much more sensitive than CBB staining. To generate a calibration curve for protein quantification, we loaded known amounts of bovine serum albumin, ovalbumin, and cytochrome *c* on one-dimensional gels, which were subsequently stained by SYPRO ruby™. Staining intensities per lane were determined by fluorimaging. Fluorescence intensities reflected the corresponding protein amounts within a deviation range of less than ±30% error determined from three gels (Fig. 2). A best-fit curve was generated and subsequently used as a calibration curve (see "Experimental Procedures"). To apply this standard calculation for further experiments, a series of known quantities (1–10 μg) of haptoglobin, a human plasma protein, was separated by 2-DE and analyzed by SYPRO ruby™ staining. Deviation of the protein amounts calculated from the sum of fluorographic intensities of all detected haptoglobin spots per gel with respect to the actually loaded protein quantities was within an error range of less than 15% of the best-fit calibration curve (data not shown).

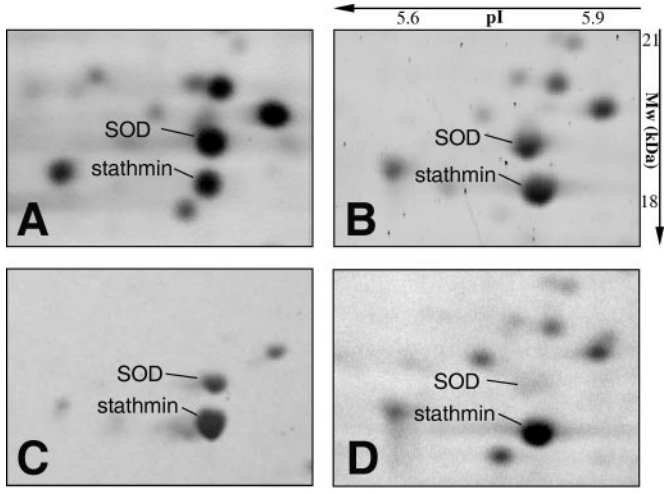

FIG. 1. **2D gel sections of radiolabeled cytosolic proteins of U937 cells.** *A*, 60 μg of protein was separated by 2D gel electrophoresis and detected by silver staining; *B*, 200 μg of protein were loaded; SYPRO ruby™ staining; *C*, 500 μg of protein were loaded; CBB-staining; *D*, autoradiograph of the SYPRO ruby™-stained gel depicted in *B*. CBB staining and SYPRO ruby™ staining provided a more reliable linearity with respect to protein amounts than silver staining, which was by far the most sensitive detection technique. Superoxide dismutase (*SOD*) was undetectable by autoradiography because of its lack in methionine.

Correlating Synthesis Rate to the Absolute Amount in Secreted Proteins—The synthesis rate of a protein can be calculated from autoradiographic measurement of the ^{35}S incorporation per unit time. 2-DE of radiolabeled proteins and subsequent phosphoimaging allowed us to determine ^{35}S incorporation rates of a large number of proteins from one gel. However, the total amount of a protein detected in a spot cannot be labeled in a uniform manner, because labeled

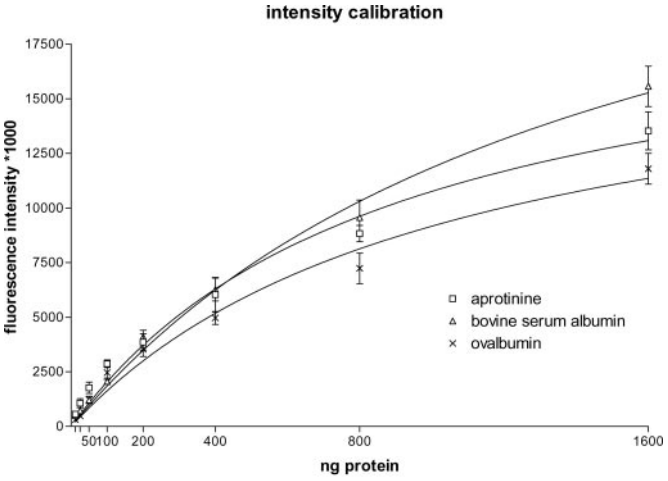

FIG. 2. **The linearity of staining intensity correlated with the protein amount.** 12.5, 25, 50, 100, 200, 400, 800, and 1600 ng of bovine serum albumin, ovalbumin, and cytochrome *c* were loaded per *lane* on one-dimensional gels and subsequently stained by SYPRO ruby™. Staining intensities per *lane* were determined by fluorimaging. *Error bars* indicate S.E. values calculated from three individual gels.

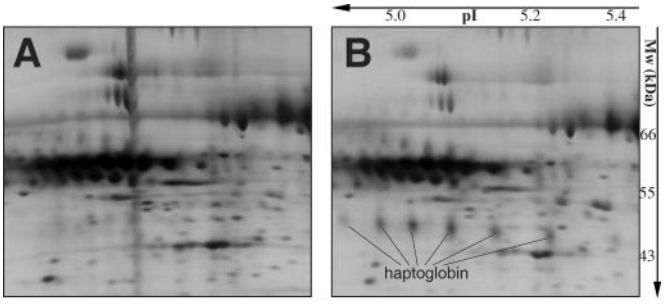

FIG. 3. **Haptoglobin secretion of HepG2 cells after IL-6 treatment.** HepG2 cells were treated with 50 ng/ml IL-6 for 24 h. Then, cells were washed and labeled with 0.2 mCi/ml [^{35}S]methionine for 1 h. Subsequently, cells were washed and subjected again to [^{35}S]methionine labeling. After 1 h, the supernatant was collected and processed for 2D gel electrophoresis. *A*, 2D ^{35}S autoradiograph section of the supernatant of untreated HepG2 cells; *B*, the corresponding ^{35}S autoradiograph section analyzing the supernatant from IL-6-pretreated HepG2 cells. Secreted haptoglobin was quantified by SYPRO ruby™ staining followed by fluorimaging, whereas ^{35}S incorporation into newly synthesized haptoglobin was determined by phosphoimaging of the same gel.

cellular proteins are composed of a mixture of unknown fractions synthesized before and during labeling. Consequently, the amount of proteins determined by *e.g.* SYPRO ruby™ staining cannot be simply related to the amount of proteins synthesized within the labeling time. The following experimental setup was designed to solve this problem.

Proteins secreted by radiolabeled cells can be easily collected by precipitation of the cell culture supernatant. Furthermore, secreted proteins can be separated repeatedly several times during culture, thereby separating labeled protein from unlabeled protein. Determination of the protein amount and corresponding autoradiograph intensity of such protein spots and considering the molecular weight and number of methionine residues per protein molecule allowed us to determine a calibration factor (CF), *i.e.* the autoradiograph spot intensity that corresponded to the incorporation of 1 nmol of ^{35}S.

Several requirements had to be fulfilled for an appropriate data evaluation. At first, we chose HepG2 cells, because they continuously secrete high amounts of plasma proteins. To avoid contamination of secreted proteins with FCS components provided by standard medium, radiolabeling was performed at serum-free culture conditions. HepG2 cells were found to cope with serum-free conditions for 2 h without any detectable cell lysis as determined by the trypan blue exclusion assay (not shown). Second, because residual FCS was still found detectable in cell supernatants after extensive washing (not shown), we chose a protein for calibration, which is generally not present in FCS. Third, we observed a lag phase of about 40 min after providing radiolabeled medium, which was required to secrete uniformly labeled proteins (not shown). Therefore, collecting protein secreted after the lag phase, a correlation of the protein amount with the corresponding autoradiograph intensity can be calculated. Finally, the amino acid sequence of the protein used for calibration has to be known to properly determine the amount of radiolabeled methionine incorporated per molecule synthesized. Furthermore, the same protein should be commercially available in purified form to calibrate SYPRO ruby™ staining. In our hands haptoglobin fulfilled all these requirements listed above and was therefore used as a calibration protein. As untreated HepG2 cells did not secrete haptoglobin, we induced the secretion of haptoglobin by treatment of HepG2 cells with IL-6 (28).

HepG2 cells were pretreated with 50 ng/ml IL-6 for 24 h and subsequently radiolabeled with [^{35}S]methionine for 1 h. Thereafter, cells were washed and incubated with fresh serum-free medium supplemented with [^{35}S]methionine for 1 h. Then the supernatant was collected, sterile-filtrated, and precipitated. The secreted proteins were separated by 2D gel electrophoresis, stained with SYPRO ruby™, and subsequently analyzed by fluorimaging and phosphoimaging, respectively. We found that 3×10^6 IL-6 pretreated HepG2 cells secreted 130 ng of haptoglobin heavy chain (sum of six spots) within 1 h, which corresponded to an autoradiograph intensity of 304,000 arbitrary units as determined by fluorimaging (median values of two experiments; see Fig. 3). Considering the five methionine residues per haptoglobin molecule and its known molecular mass of 38.5 kDa, we determined the CF as 18,000 $\pm$ 3,200 arbitrary autoradiograph units (error calculated from individual spots) corresponding to the incorporation of 1 pmol of ^{35}S.

Application of the Calibration Factor for Determination of Synthesis Rates of Intracellular Proteins—Having determined the CF to calculate ^{35}S incorporation from the autoradiograph intensity of any 2D spot under consideration, we were able to calculate absolute synthesis rates for intracellular proteins as follows: SR [ng/h $\times$ 10^6 cells] = $AR_{PI} \times Mw/(CF \times t_{label} \times$

n_{Mcells}), where *SR* is synthesis rate, AR_{PI} is the number of ^{35}S autoradiograph units determined by phosphoimaging of a spot divided by the number of methionines per molecule, *Mw* is the molecular mass of the protein in Dalton, *CF* is calibration factor (18,000 arbitrary autoradiograph units per 1 pmol of ^{35}S), t_{label} is the labeling time in h, and n_{Mcells} is the number of cells divided by one million corresponding to the amount of protein loaded onto the gel.

To check the accuracy of this method, we performed a heat shock experiment. Heat shock of cells is a stimulus, which has been well demonstrated to induce synthesis of a group of proteins, designated as heat shock proteins (29). Thus we intended to independently determine protein amounts and the corresponding synthesis rates during a heat shock time course experiment. In case the CF was determined correctly, the two independently determined measurements should fit, *i.e.* integration of the calculated synthesis rates should reflect the observed increase in protein amounts determined by SYPRO ruby™ staining.

To assess the specificity of induction of protein synthesis, U937 were heat-shocked for 7 min at 44 °C and subsequently cultivated for another 2 h. Then, cells were radiolabeled for 2 h, harvested, fractionated, and forwarded to proteome analysis. As shown in Fig. 4, the synthesis rates of most proteins resolved by this technique, including actin, calreticulin, α-enolase, endoplasmic reticulum protein ER-60, initiation factor 5A, phosphoglycerate mutase, and stathmin were almost uniformly decreased, whereas the synthesis rates of hsps 110, 70, 70B, 60, 57, and 27 were found increased dramatically.

For the quantitative analysis of the time course experiment the heat shock was performed for 10 min at 43 °C. U937 were heat-shocked, further cultivated for 2, 6, and 10 h and subsequently radiolabeled for 2 h. Control cells were radiolabeled for 2 h and either not heat-shocked or heat-shocked after labeling and harvested directly afterward. RNA was isolated from unlabeled cell aliquots treated alike and used for Northern analysis. Fig. 5 shows alterations of hsp70 protein level, synthesis rate, and gene transcription during the time course experiment. Although the hsp70 synthesis rate of untreated U937 cells as calculated from phosphoimaging was 8 ng per h per 10^6 cells, 4 h after heat shock the synthesis rate was increased to 170 ng per h per 10^6 cells (see Fig. 5 and Fig. 6). As the labeling time was 2 h each, these data represent an averaged synthesis performance, respectively. For integration of the synthesis rate, we considered a lag phase of 1 h until cells achieved the synthesis performance and connected the obtained data points in a linear manner (Fig. 7). Thus we calculated an absolute amount of hsp70 of about 480 ng synthesized within these 4 h (Fig. 7). This corresponded well to the observed increase from 110 ng of hsp70/10^6cells to 500 ng of hsp70/10^6cells after that period of time (Fig. 6). 8 h after the heat shock, the synthesis rate was found decreased to a value only little above untreated cells, whereas the present amount of hsp70 had accumulated to 650 ng/10^6 cells

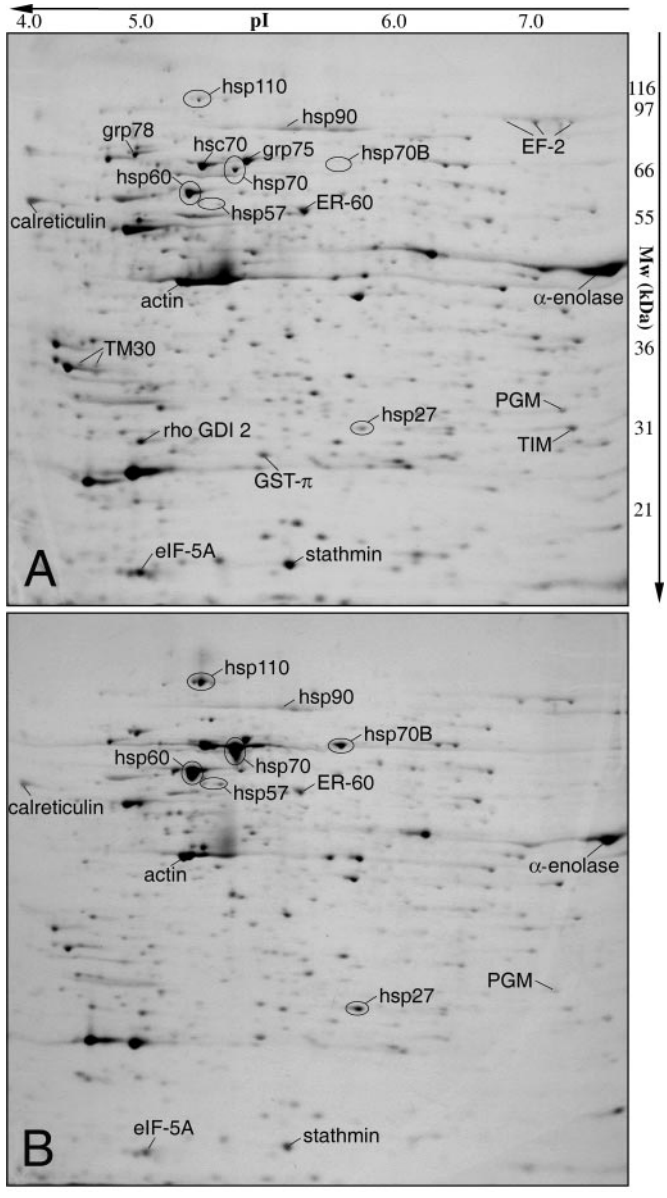

FIG. 4. **Proteome alterations in response to heat shock.** U937 were heat-shocked for 7 min at 44 °C and cultured for 2 h at 37 °C. Thereafter, cells were radiolabeled for 2 h with 0.2 mCi/ml [^{35}S]methionine. Subsequently, cytosolic proteins were extracted and processed for 2D gel electrophoresis as described under "Experimental Procedures." Control cells were treated alike without heat shock. *A*, 2D autoradiograph of cytosolic proteins isolated from control U937 cells; *B*, the corresponding 2D autoradiograph in heat-shocked U937 cells. Proteins were identified by 2D Western blotting and mass spectrometry analysis as reported previously (18, 32). Note the specific induction of heat shock proteins synthesis (*circled*), whereas the production of essentially all other proteins detected was rather decreased. Some landmark proteins are annotated. *EF-2*, elongation factor 2; *eIF-5A*, initiation factor 5A; *grp75/78*, 75/78 kDa glucose-regulated protein; *GST-π*, glutathione *S*-transferase π; *PGM*, phosphoglycerate mutase; *rho GDI 2*, Rho GDP-dissociation inhibitor 2; *TM30*, tropomyosin α-chain; *TIM*, triosephosphate isomerase (see Table I for SwissProt accession numbers).

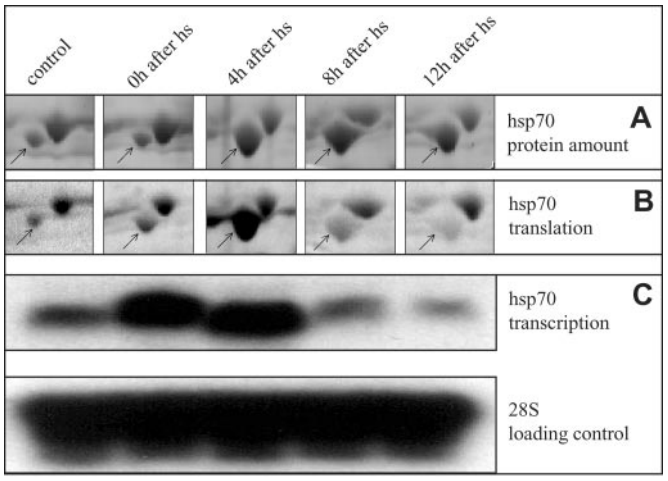

FIG. 5. **Alterations in transcription, translation, and protein amount of hsp70 after heat shock.** Control U937 cells were not heat-shocked or heat-shocked directly after labeling and then processed. U937 cells were heat-shocked for 10 min at 43 °C. After 2, 6, and 10 h cells were labeled for another 2 h with [^{35}S]methionine and forwarded to proteome analysis. RNA was isolated from unlabeled cells treated identically otherwise. *A*, 2D gel section showing hsp70 stained with SYPRO ruby™, reflecting protein amounts; *B*, phosphoimaging of corresponding gel sections reflecting synthesis rates; *C*, expression of hsp70 and 28 S RNA as loading control. Cytoplasmic RNA was prepared and analyzed by Northern blotting as outlined under "Experimental Procedures." *Arrows* indicate hsp70 protein. Note that the *spot* located to the *upper right* of hsp70, corresponding to glucose-regulated protein 75, was essentially unchanged during the heat shock experiment. Data are from one representative experiment.

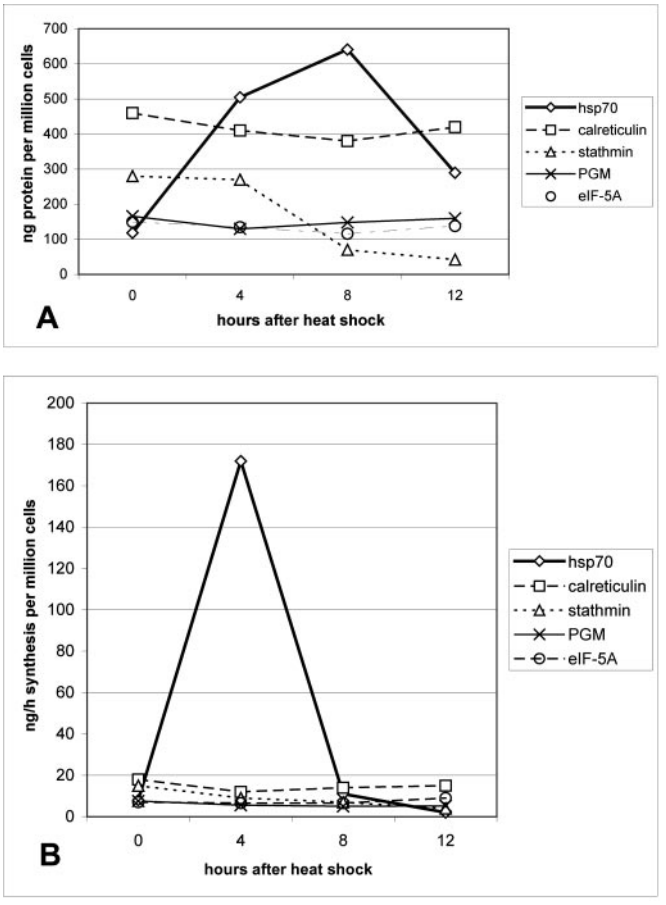

FIG. 6. **Protein quantification and synthesis rates during heat shock kinetics.** Protein amounts were quantified by fluorography of SYPRO ruby™ staining, whereas synthesis rates were calculated from radiolabeled spot intensities as outlined in the text. *A*, absolute values of individual proteins; *B*, absolute synthesis rates of proteins. Data are from one representative experiment.

(Figs. 5 and 6). Intriguingly, after 12 h, the hsp70 synthesis rate dropped to 25% of the control level, accompanied by a decrease of hsp70 amount to less than 300 ng/10^{6}cells (Figs. 5 and 6). This finding indicated clearly the specific induction of degradation of hsp70. Combination of Northern and proteome analysis allowed us to investigate the relation of transcription with the corresponding protein translation. As demonstrated in Fig. 5*C*, hsp70 transcription was found strongly induced immediately after heat shock, whereas, as expected, the translation rate was essentially unchanged. Hsp70 transcription remained high after 4 h and dropped below control levels after 8 and 12 h. Evidently, after the lag phase required for onset of new protein synthesis, the synthesis rate was found strictly according to the transcription rate. This result pointed to a transcriptional control of hsp70 synthesis as has been suggested earlier (30).

During the whole time course investigated after heat shock, synthesis rates of other proteins were found decreased slightly, essentially recovering to control levels after 12 h (Fig. 6). Stathmin was found to be much more affected than other proteins (Fig. 6 provides representative examples). Because stathmin has been described to be phosphorylated upon heat shock (31), and we could not find accumulation of the phosphorylated isoform, our findings suggested that the phosphorylated isoform might become degraded subsequently.

Calculating the Turnover Rate of Proteins by Determination of Absolute Protein Amounts and Synthesis Rates—Two independent sets of data were collected of each SYPRO ruby™-stained gel of radiolabeled proteins; fluorimaging allowed us to determine the absolute amount of any protein resolved in a 2D-gel, whereas phosphoimaging provided the amount of ^{35}S incorporated per spot per unit of time. Availability of absolute protein amounts in combination with synthesis rates made it easy to calculate the time theoretically required to synthesize the measured amount of any detectable protein. Assuming a steady state of protein turnover, the time required to synthesize a cellular protein equals the time to degrade it. Hence, half of this synthesis time corresponds to the biological half-life of a protein. In the case of proliferating cells, the contribution to the gain of mass was subtracted from the protein synthesis performance, resulting in the synthesis rate required to compensate protein degradation. Thus, half-lives of proteins were calculated as follows:

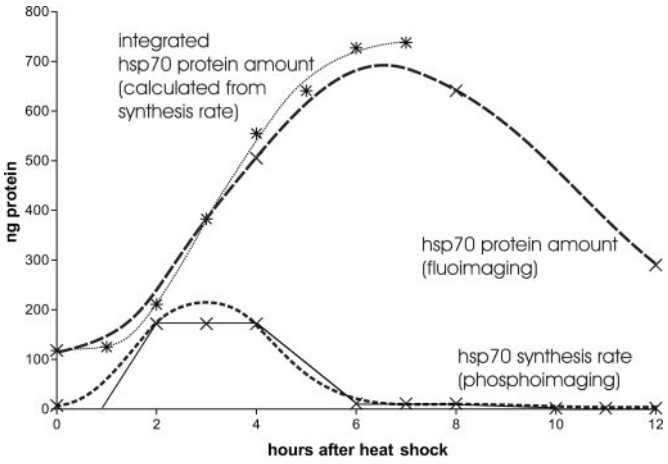

FIG. 7. **Integration of synthesis rates closely reflects accumulated hsp70 levels.** Levels indicated at the *y*-axis refer to synthesis rates (ng/hour) and protein amounts (ng). *Fitted curves* were drawn through the experimentally determined data points (x) to better represent a realistic perspective. Integration of the synthesis rates of hsp70 (*, calculated data points) allowed us to determine cumulative levels and thus to correlate them to the actually observed levels. The integration curve was found close to the experimentally determined protein amounts; however, induction of specific protein degradation of hsp70 after several hours seems evident. Therefore, the calculated curve of hsp70 accumulation was terminated at 7 h after heat shock. Data are from one representative experiment.

$t_{1/2} = (A_{total}/2)/((SR \times t_{dupl} - A_{total})/t_{dupl})$, where $t_{1/2}$ is biological half-life, A_{total} is absolute protein amount, *SR* is synthesis rates of respective protein, and t_{dupl} is duplication time of cells (29.5 h in the presented experiment).

To validate this approach, we determined protein half-lives by an independent method, *i.e.* pulse-chase experiments, which proved useful for investigation of protein turnover by proteome analysis (23). We pulsed two aliquots of untreated U937 cells for 2 h at our standard conditions; one aliquot was harvested immediately, whereas the other was washed and chased for 24 h. Subsequent proteome analysis provided autoradiograph intensities for protein spots of interest determined by phosphoimaging at time 0 (ARt_0) and at 24 h thereafter (ARt_{24}). These values were corrected for the net growth of cells in the given time period, and the half-lives of proteins was calculated as follows: $t_{1/2} = -24 \times \log2/\log(ARt_{24}/ARt_0)$, where ARt_0 is autoradiograph intensity of a protein after pulsing the cells, and ARt_{24} is autoradiograph intensity of a protein after pulsing and subsequently chasing the cells for 24 h.

Autoradiograph intensity values were normalized with respect to the protein amount of the corresponding spots as determined by fluorography. In the following we compared protein half-lives determined independently by each of the two methods. Biological half-lives of 15 proteins (indicated in Fig. 4), which we have identified previously (18, 32), were calculated using the fluorimaging and phosphoimaging data and compared with the corresponding values obtained from pulse-chase experiments (see Table I). Although the median protein half-life was found to be about 32 h in U937 cells, by both methods we determined the same set of proteins with rather long half-lives, such as calreticulin (66.5 and 65.3 h, respectively; see Table I), and proteins with apparently much higher turnover rates, such as hsp70 (half-life 16.4 and 20.0 h, respectively; see Table I). These data suggested that concomitant quantification of protein amounts and synthesis rates allows easy and reliable calculation of biological half-lives of proteins.

DISCUSSION

We describe a novel strategy for quantitative proteome profiling, which for the first time provided the means to determine absolute values of protein amounts, synthesis rates, and turnover rates for known proteins resolved by 2-DE. The method is based on electrophoretic separation of protein fractions isolated from metabolically labeled cells and quantitative analysis of 2D gels by both fluorimaging and phosphoimaging. Thereby, two independent sets of data were obtained as read-outs of each single gel. Calibration of the autoradiograph intensity, using a secreted protein as a reference, allowed us to directly determine synthesis rates of known intracellular proteins resolved by 2D autoradiography. In addition, we demonstrated that protein turnover rates could be calculated from the relation of the amount of a protein to its synthesis rates. This was based on the assumption that the synthesis rate of proteins in a steady state of cell metabolism would essentially compensate protein degradation and was corrected considering the net gain of protein mass by cell duplication in proliferating cells. This novel straightforward approach resulted in a comprehensive survey of biological parameters (protein amounts, synthesis rates, and turnover rates) for any identified protein by dual analysis of a single 2D gel and application of bioinformatic tools.

Optimizing absolute protein quantification by itself will prove to become a very useful tool. Recently, we demonstrated that altered protein amounts of some marker proteins detected in plasma of cancer patients were related to hypercoagulation and interference with cell death induction (33, 34). Determination of quantitative proteome profiles of human plasma protein samples may allow us to identify patterns of quantitative alterations characteristic for certain diseases such as cancer. Preliminary data of quantitative proteome analysis of immunoprecipitated protein complexes suggested that this method might help to determine the stoichiometry of such complexes and should also provide information to identify unspecific interactions.[2]

However, several general requirements had to be fulfilled to reliably calculate absolute measures from fluorimaging and phosphoimaging. Obviously, during the whole procedure, including protein isolation and protein separation by 2-DE, protein loss had to be strictly avoided. Therefore, we designed a subcellular fractionation protocol in a manner to prevent any

[2] C. Gerner, unpublished data.

TABLE I

Biological half-lives of individual proteins in U937 cells determined by calculations from protein amounts and synthesis rates in comparison to pulse-chase experiments

FI, as determined by fluorimaging; PI, as determined by phosphoimaging. S.E. values of protein amounts, synthesis rates, and biological half-lives determined from pulse-chase experiments were obtained from three individual experiments, and error values of calculated biological half-lives were calculated combining the error rates of protein amounts and synthesis rates, respectively.

Protein	SwissProt accession no.	ng of protein per 10^6 cells (FI)	Synthesis in ng/h per 10^6 cells (PI)	Theoretical time required for synthesis	Calculated biological half-life	Autoradiograph intensity recovered after pulse-chase *vs.* control	Biological half-life determined from pulse-chase
				h	*h*	%	*h*
hsp70	P08107	118 ± 11	7.2 ± 0.62	16.4	18.1 ± 3.3	43.5	20.0 ± 1.6
Calreticulin	P27797	460 ± 62	18.8 ± 0.28	24.5	66.5 ± 19	77.5	65.3 ± 7.2
Stathmin	P16949	280 ± 13	14.3 ± 0.84	19.6	28.2 ± 3.0	56.3	28.9 ± 2.2
PGM	P18669	166 ± 10	8.2 ± 0.37	20.2	32.4 ± 3.6	63.5	36.6 ± 3.6
eIF-5A	P10159	150 ± 17	7.0 ± 0.41	21.4	37.5 ± 6.5	60.8	33.4 ± 4.4
TIM	P00938	345 ± 37	17.1 ± 1.2	20.2	31.0 ± 5.4	55.5	28.3 ± 2.2
ER-60	P27797	136 ± 29	8.1 ± 1.5	16.0	19.2 ± 6.7	45.6	21.2 ± 2.3
EF-2	P13639	224 ± 16	11.4 ± 1.1	19.6	28.3 ± 4.7	52.8	26.0 ± 3.1
GST-π	P09211	540 ± 23	25.4 ± 1.6	21.2	36.4 ± 3.8	66.0	40.0 ± 2.8
hsc70	P11142	915 ± 71	48.4 ± 6.1	18.9	25.6 ± 5.2	47.2	22.2 ± 2.4
grp75	P38646	295 ± 28	14.5 ± 1.9	20.3	31.6 ± 7.2	56.1	28.8 ± 3.0
grp78	P11021	325 ± 49	16.5 ± 1.8	19.7	28.8 ± 7.5	61.6	34.4 ± 4.2
TM30	P07226	132 ± 25	6.2 ± 1.0	21.3	37.0 ± 13	60.8	33.4 ± 2.9
hsp60	Q9POX2	320 ± 19	15.7 ± 1.1	20.4	31.8 ± 4.2	60.0	32.5 ± 1.9
rho GDI 2	P52566	185 ± 15	9.3 ± 0.9	19.9	29.2 ± 5.2	55.3	28.0 ± 1.6

potential loss of cellular proteins (see "Experimental Procedures"). During separation of proteins by isoelectric focusing, protein might be lost by unspecific precipitation. Analysis of the residual proteins that do not enter the gel system after isoelectric focusing suggested that no unspecific precipitation occurred under the conditions we used (see "Experimental Procedures"). Interestingly, this was only true for isolated subcellular protein fractions, which had been introduced to optimize spot resolution and minimize background of gels but not for whole cell samples (data not shown). However, the distribution of a protein among different protein fractions required that the contribution to each fraction had to be considered for correct quantification. This was achieved by the simple addition of the amounts found in the cytosol, as well as in the pelleted cytoplasmic protein fraction. Another potential loss of protein, which might occur during transfer of the first dimension tube gel to the second dimension SDS gel, was avoided by equilibration of the tube gel on top of the SDS gel, not removing the equilibration buffer at all. Very little to undetectable staining intensity of the tube gel by silver staining suggested that essentially all protein migrated into the gel (data not shown). Having available the absolute amounts of all protein spots on a 2D gel determined by fluorography, we were able to compare the sum of those to the amount of protein loaded onto the gel, which was determined by a conventional protein assay (data not shown). Within the resolved molecular mass range from about 15 to 200 kDa and a pI range from 3.5 to 8.0 the sum of protein spots reached ~55% of the amount of protein loaded onto a gel (data not shown). Considering proteins not represented within these limits, this result again suggested that essentially all proteins loaded onto a 2D gel entered the gel system successfully.

Another requirement to assess absolute measures was the identification of proteins on 2D gels, as the number of methionines per molecule has to be known. Certain proteins, such as haptoglobin, exist in various post-translational isoforms, which are represented by several spots on a 2D gel. Protein isoforms are usually identified by 2D Western blotting. For correct quantification, all protein isoforms have to be taken into consideration. Unrecognized protein isoforms would consequently result in incorrect quantification of the corresponding protein. On the other hand, quantification of known protein isoforms allowed us to calculate quantitative changes between post-transcriptional modifications of proteins. Investigation of post-transcriptional modifications of proteins indeed represents another important feature of proteome profiling.

To our knowledge, this is the fist time a method was presented to determine absolute values for protein synthesis rates of a large number of proteins. Evidently many potential causes for errors exist as outlined above. The precision of the method relies on the general reproducibility of 2D pattern, as well as on the precision of fluorography and phosphoimaging. Following the conditions to strictly avoid unspecific protein precipitation during 2D electrophoresis generally allowed us to optimize the reproducibility of 2D protein patterns, which was also achieved in the case of highly insoluble nuclear proteins (32, 35, 36). However, the main precision limit was posed by the accuracy of protein quantification by SYPRO ruby™ staining. Several techniques have been developed to enhance SYPRO ruby™ staining allowing subsequent mass

spectrometry analysis (22). To enhance the staining sensitivity and linearity, we have introduced a protein cross-linking step prior to staining (see "Experimental Procedures"), which renders subsequent mass spectrometry analysis impossible. As a result from cross-linking, essentially all proteins detectable by autoradiography were also well detectable by SYPRO ruby™ staining, suggesting that any cytoplasmic protein of sufficient abundance may be quantified applying this technique (not shown). However, our fluorimaging calibration data (Fig. 2) suggested that an error rate of ~30% with respect to absolute protein amounts has to be taken into consideration.

So far, pulse-chase experiments were used as a standard technique to monitor protein turnover of a large number of proteins. Successful application of this approach requires a steady state of cell metabolism during an extended time period, which hardly applies to short term treatments (*e.g.* heat shock, immediate drug responses). The method devised presently will enable assessment of regulation of turnover rates taking place within short time periods. Monitoring of protein half-lives in profiling experiments may be of similar significance as monitoring protein amounts and synthesis rates, as regulated protein degradation (37) has been demonstrated to play key roles in various physiological processes such as cell cycle (38), differentiation (39), aging (40, 41), and carcinogenesis (42).

Generating proteome profiles of cells in response to a specific stimulus becomes comprehensive by the introduction of subcellular fractionation in addition to metabolic labeling. During Fas-induced apoptosis of Jurkat cells, we observed proteome alterations, which we were able to interpret as consequences of protein modification, translocation, induced synthesis, degradation, or aggregation (18, 36). Extending the presently described quantification techniques with these techniques therefore provides the means to even more comprehensively dissect and profile cellular proteome alterations, in a best-case scenario for any cellular system available.

Combination of quantitative proteome profiling with gene expression profiling may be helpful to better understand physiological processes and their underlying regulatory mechanisms. As shown recently, analysis of both transcriptional and translational regulation has been accomplished by differential screening using ribosome-free and ribosome-bound mRNA (6). In combination with quantitative proteome data, these techniques will allow us to gain comprehensive insights into complex regulatory events by monitoring steady state mRNA levels, protein abundance, synthesis, and turnover.

* The costs of publication of this article were defrayed in part by the payment of page charges. This article must therefore be hereby marked "*advertisement*" in accordance with 18 U.S.C. Section 1734 solely to indicate this fact.

‡ To whom correspondence should be addressed: The Smurfit Institute of Genetics, Trinity College, Dublin 2, Ireland. Tel.: 353-1-6081089; Fax: 353-1-6798558; E-mail: Christopher.Gerner@univie.ac.at.

REFERENCES

1. Celis, J. E., Kruhoffer, M., Gromova, I., Frederiksen, C., Ostergaard, M., Thykjaer, T., Gromov, P., Yu, J., Palsdottir, H., Magnusson, N., and Orntoft, T. F. (2000) Gene expression profiling: monitoring transcription and translation products using DNA microarrays and proteomics. *FEBS Lett.* **480,** 2–16
2. Gygi, S. P., Rochon, Y., Franza, B. R., and Aebersold, R. (1999) Correlation between protein and mRNA abundance in yeast. *Mol. Cell. Biol.* **19,** 1720–1730
3. Pradet-Balade, B., Boulme, F., Beug, H., Mullner, E. W., and Garcia-Sanz, J. A. (2001) Translation control: bridging the gap between genomics and proteomics? *Trends Biochem. Sci.* **26,** 225–229
4. Lipshitz, H. D., and Smibert, C. A. (2000) Mechanisms of RNA localization and translational regulation. *Curr. Opin. Genet. Dev.* **10,** 476–488
5. Guhaniyogi, J., and Brewer, G. (2001) Regulation of mRNA stability in mammalian cells. *Gene* **265,** 11–23
6. Mikulits, W., Pradet-Balade, B., Habermann, B., Beug, H., Garcia-Sanz, J. A., and Mullner, E. W. (2000) Isolation of translationally controlled mRNAs by differential screening. *FASEB J.* **14,** 1641–1652
7. Sonenberg, N., Hershey, J. W. B., and Mathews, M. B. (2000) *Translational Control of Gene Expression*. *Cold Spring Harbor Monograph Series*, Cold Spring Harbor Laboratory Press, Cold Spring Harbor, NY
8. Bochtler, M., Ditzel, L., Groll, M., Hartmann, C., and Huber, R. (1999) The proteasome. *Annu. Rev. Biophys. Biomol. Struct.* **28,** 295–317
9. Fung, E. T., Thulasiraman, V., Weinberger, S. R., and Dalmasso, E. A. (2001) Protein biochips for differential profiling. *Curr. Opin. Biotechnol.* **12,** 65–69
10. Jenkins, R. E., and Pennington, S. R. (2001) Arrays for protein expression profiling: towards a viable alternative to two-dimensional gel electrophoresis? *Proteomics* **1,** 13–29
11. Unlu, M., Morgan, M. E., and Minden, J. S. (1997) Difference gel electrophoresis: a single gel method for detecting changes in protein extracts. *Electrophoresis* **18,** 2071–2077
12. Tonge, R., Shaw, J., Middleton, B., Rowlinson, R., Rayner, S., Young, J., Pognan, F., Hawkins, E., Currie, I., and Davison, M. (2001) Validation and development of fluorescence two-dimensional differential gel electrophoresis proteomics technology. *Proteomics* **1,** 377–396
13. Oda, Y., Huang, K., Cross, F. R., Cowburn, D., and Chait, B. T. (1999) Accurate quantitation of protein expression and site-specific phosphorylation. *Proc. Natl. Acad. Sci. U. S. A.* **96,** 6591–6596
14. Regnier, F. E., Riggs, L., Zhang, R., Xiong, L., Liu, P., Chakraborty, A., Seeley, E., Sioma, C., and Thompson, R. A. (2002) Comparative proteomics based on stable isotope labeling and affinity selection. *J. Mass Spectrom.* **37,** 133–145
15. Gygi, S. P., Rist, B., Gerber, S. A., Turecek, F., Gelb, M. H., and Aebersold, R. (1999) Quantitative analysis of complex protein mixtures using isotope-coded affinity tags. *Nat. Biotechnol.* **17,** 994–999
16. Cagney, G., and Emili, A. (2002) *De novo* peptide sequencing and quantitative profiling of complex protein mixtures using mass-coded abundance tagging. *Nat. Biotechnol.* **20,** 163–170
17. Smolka, M., Zhou, H., and Aebersold, R. (2002) Quantitative protein profiling using two-dimensional gel electrophoresis, isotope-coded affinity tag labeling, and mass spectrometry. *Mol. Cell. Proteomics* **1,** 19–29
18. Gerner, C., Frohwein, U., Gotzmann, J., Bayer, E., Gelbmann, D., Bursch, W., and Schulte-Hermann, R. (2000) The Fas-induced apoptosis analyzed by high throughput proteome analysis. *J. Biol. Chem.* **275,** 39018–39026
19. Gygi, S. P., and Aebersold, R. (1999) Absolute quantitation of 2-D protein spots. *Methods Mol. Biol.* **112,** 417–421
20. Steinberg, T. H., Jones, L. J., Haugland, R. P., and Singer, V. L. (1996) SYPRO orange and SYPRO red protein gel stains: one-step fluorescent staining of denaturing gels for detection of nanogram levels of protein. *Anal. Biochem.* **239,** 223–237
21. Lopez, M. F., Berggren, K., Chernokalskaya, E., Lazarev, A., Robinson, M., and Patton, W. F. (2000) A comparison of silver stain and SYPRO Ruby Protein Gel Stain with respect to protein detection in two-dimensional gels and identification by peptide mass profiling. *Electrophoresis* **21,** 3673–3683
22. Berggren, K. N., Schulenberg, B., Lopez, M. F., Steinberg, T. H., Bogdanova, A., Smejkal, G., Wang, A., and Patton, W. F. (2002) An improved formulation of SYPRO Ruby protein gel stain: Comparison with

the original formulation and with a ruthenium II tris (bathophenanthroline disulfonate) formulation. *Proteomics* **2,** 486–498
23. Rodemann, H. P. (1990) Degradation of individual intracellular proteins analyzed by two-dimensional gel electrophoresis and computerized video densitometry. *Electrophoresis* **11,** 228–231
24. Wray, W., Boulikas, T., Wray, V. P., and Hancock, R. (1981) Silver staining of proteins in polyacrylamide gels. *Anal. Biochem.* **118,** 197–203
25. Mikulits, W., Hengstschlager, M., Sauer, T., Wintersberger, E., and Mullner, E. W. (1996) Overexpression of thymidine kinase mRNA eliminates cell cycle regulation of thymidine kinase enzyme activity. *J. Biol. Chem.* **271,** 853–860
26. Wu, B., Hunt, C., and Morimoto, R. (1985) Structure and expression of the human gene encoding major heat shock protein HSP70. *Mol. Cell. Biol.* **5,** 330–341
27. Mikulits, W., Sauer, T., Infante, A. A., Garcia-Sanz, J. A., and Mullner, E. W. (1997) Structure and function of the iron-responsive element from human ferritin L chain mRNA. *Biochem. Biophys. Res. Commun.* **235,** 212–216
28. Derfalvi, B., Igaz, P., Fulop, K. A., Szalai, C., and Falus, A. (2000) Interleukin-6-induced production of type II acute phase proteins and expression of junB gene are down-regulated by human recombinant growth hormone in vitro. *Cell Biol. Int.* **24,** 109–114
29. Morimoto, R. I., Kline, M. P., Bimston, D. N., and Cotto, J. J. (1997) The heat-shock response: regulation and function of heat-shock proteins and molecular chaperones. *Essays Biochem.* **32,** 17–29
30. Liu, R. Y., Corry, P. M., and Lee, Y. J. (1994) Regulation of chemical stress-induced hsp70 gene expression in murine L929 cells. *J. Cell Sci.* **107,** 2209–2214
31. Beretta, L., Dubois, M. F., Sobel, A., and Bensaude, O. (1995) Stathmin is a major substrate for mitogen-activated protein kinase during heat shock and chemical stress in HeLa cells. *Eur. J. Biochem.* **227,** 388–395
32. Gerner, C., Holzmann, K., Meissner, M., Gotzmann, J., Grimm, R., and Sauermann, G. (1999) Reassembling proteins and chaperones in human nuclear matrix protein fractions. *J. Cell. Biochem.* **74,** 145–151
33. Gerner, C., Steinkellner, W., Holzmann, K., Gsur, A., Grimm, R., Ensinger, C., Obrist, P., and Sauermann, G. (2001) Elevated plasma levels of crosslinked fibrinogen gamma-chain dimer indicate cancer-related fibrin deposition and fibrinolysis. *Thromb. Haemost.* **85,** 494–501
34. Vejda, S., Posovszky, C., Zelzer, S., Peter, B., Bayer, E., Gelbmann, D., Schulte-Hermann, R., and Gerner, C. (2002) Plasma from cancer patients featuring a characteristic protein composition mediates protection against apoptosis. *Mol. Cell. Proteomics* **1,** 387–393
35. Gerner, C., Holzmann, K., Grimm, R., and Sauermann, G. (1998) Similarity between nuclear matrix proteins of various cells revealed by an improved isolation method. *J. Cell. Biochem.* **71,** 363–374
36. Gerner, C., Gotzmann, J., Frohwein, U., Schamberger, C., Ellinger, A., and Sauermann, G. (2002) Proteome analysis of nuclear matrix proteins during apoptotic chromatin condensation. *Cell Death Differ.* **9,** 671–681
37. Beynon, R. J., and Bond, J. S. (1986) Catabolism of intracellular protein: molecular aspects. *Am. J. Physiol.* **251,** 141–152
38. Welch, P. J., and Wang, J. Y. (1992) Coordinated synthesis and degradation of cdc2 in the mammalian cell cycle. *Proc. Natl. Acad. Sci. U. S. A.* **89,** 3093–3097
39. Mohanty, S., Lee, S., Yadava, N., Dealy, M. J., Johnson, R. S., and Firtel, R. A. (2001) Regulated protein degradation controls PKA function and cell-type differentiation in Dictyostelium. *Genes Dev.* **15,** 1435–1448
40. Goto, S., Takahashi, R., Kumiyama, A. A., Radak, Z., Hayashi, T., Takenouchi, M., and Abe, R. (2001) Implications of protein degradation in aging. *Ann. N. Y. Acad. Sci.* **928,** 54–64
41. Ryazanov, A. G., and Nefsky, B. S. (2002) Protein turnover plays a key role in aging. *Mech. Ageing Dev.* **123,** 207–213
42. Pajonk, F., and McBride, W. H. (2001) The proteasome in cancer biology and treatment. *Radiat. Res.* **156,** 447–459